SIAM J. Applied Dynamical Systems
Vol. 2, No. 4, pp. 647–671

Pulse Dynamics in an Actively Mode-Locked Laser*

John B. Geddes†, Willie J. Firth‡, and Kelly Black§

Abstract. We consider pulse formation dynamics in an actively mode-locked laser. We show that an amplitude-modulated laser is subject to large transient growth and we demonstrate that at threshold the transient growth is precisely the Petermann excess noise factor for a laser governed by a nonnormal operator. We also demonstrate an exact reduction from the governing PDEs to a low-dimensional system of ODEs for the parameters of an evolving pulse. A linearized version of these equations allows us to find analytical expressions for the transient growth below threshold. We also show that the nonlinear system collapses onto an appropriate fixed point, and thus in the absence of noise the ground-mode laser pulse is stable. We demonstrate numerically that, in the presence of a continuous noise source, however, the laser destabilizes and pulses are repeatedly created and annihilated.

Key words. mode-locked laser, transient growth, excess noise, Hermite polynomials

AMS subject classifications. 37-xx, 35-xx

DOI. 10.1137/S1111111102416599

1. Introduction.

Lasers play a crucial role in a number of optical devices and technologies. They are at the core of various consumer devices, and they are responsible for the rate of increase in the speed of our optical communication networks [20]. The need for stable pulsed lasers continues, and this continues to fuel research into either improving current devices or inventing new ones [37].

While the variety of lasers on the marketplace today is quite astounding, a typical laser is composed of an optical resonator, a laser gain medium, and a pump source [33]. The resonator can in principle support a large number of longitudinal (along the resonator axis) and transverse (transverse to the resonator axis) modes. The resonator also introduces losses, which are frequency-dependent. The frequency band over which laser oscillation can occur is determined by the frequency region over which the gain of the laser medium exceeds the resonator losses.

In terms of the longitudinal modes, most lasers have many modes within the gain band, and the laser output consists of radiation at a number of closely spaced frequencies. In the absence of any further control elements, random fluctuations and nonlinear effects in the laser result in an output that varies in an unpredictable way. If, on the other hand, the oscillating modes are forced to maintain equal frequency spacing and a fixed phase relationship, it is possible

*Received by the editors October 30, 2002; accepted for publication (in revised form) by C. Jones July 2, 2003; published electronically December 22, 2003. A preliminary report of the results presented here was given at the IQEC/CLEO Europe in Nice, France in September 2000 (paper CThJ 0007) and at the SIAM Conference on Applications of Dynamical Systems in Snowbird, Utah in May 2001 (session CP25).
http://www.siam.org/journals/siads/2-4/41659.html
†Franklin W. Olin College of Engineering, Needham MA 02492 (john.geddes@olin.edu).
‡Department of Physics, University of Strathclyde, Glasgow G4 0NG, Scotland (willie@phys.strath.ac.uk).
§Department of Mathematics and Statistics, University of New Hampshire, Durham NH 03824 (kelly.black@unh.edu).

to obtain a variety of mode-locked behaviors, including a frequency-modulated output and a continuous train of laser pulses. The technique of mode-locking was proposed theoretically by Lamb in 1964 [25].

In the same year a number of experimental studies were published on the use of internal modulation to obtain mode-locking in gas lasers. Hargrove, Fork, and Pollack [16] experimentally obtained a train of pulses from an He-Ne laser by mode-locking with an internal acoustic loss modulator. Harris and Targ [17] used an internal frequency modulator to mode-lock the same laser, resulting in a frequency-modulated output. In the following years, the techniques of mode-locking were demonstrated in other laser systems, including the argon ion laser [7], the ruby laser [4], and the neodymium-doped yttrium aluminum garnet (Nd:YAG) laser [6]. In each case, the pulse-widths achieved were on the order of tens of pico-seconds, but the pulse trains were subject to fluctuations and instabilities. Other means of mode-locking were also employed, including self-locking [3] and the use of saturable absorbers [8].

Theoretical work on active mode-locking developed in concert with experimental work, with emphasis on either internal amplitude modulation (AM) or frequency modulation (FM). DiDomenico [5] showed theoretically that mode-locking could be obtained by internal loss modulation, while Harris and McDuff [18] developed an internal FM theory. Haken and Pauthier [15] showed later that mode-locked laser pulses are described by a harmonic-oscillator eigenfunction. Nelson [29] extended this work and showed that the steady-state laser pulse is described by a Gaussian envelope modulated by polynomials. These efforts were all carried out in the frequency domain.

The first theoretical results in the time domain were obtained by Kuizenga and Siegman [23], who were able to predict the width of mode-locked pulses in AM and FM lasers. These predictions were confirmed experimentally by the same authors for FM laser operation [24] and by Smith et al. [36] for an AM laser. The theory of Kuizenga and Siegman was based on the assumption that a circulating Gaussian pulse exists in the resonator. By imposing a self-consistency condition after one round-trip, they showed in a simple way that a steady-state Gaussian pulse could exist. Kim, Marathe, and Rabson [22] later showed that the Gaussian pulse was in fact a solution of an integral equation and that higher-order solutions also existed—the Hermite–Gaussian modes. Haus [19] demonstrated two years later that the higher-order modes are linearly unstable and hence unrealizable in the steady-state.

The technique of internal modulation introduces two parameters—the depth of the modulation and the degree to which the modulation period is detuned from the round-trip time of the laser cavity. While the steady-state effects of detuning were considered in the early years of mode-locked lasers, it is only more recently that the dynamic effects of detuning have come under scrutiny. In 1998, Morgner and Mitschke [27] investigated the influence of detuning on the pulse formation dynamics in mode-locked lasers. They found experimentally that in an actively mode-locked laser the equilibrium position of the laser pulse shifts linearly with respect to the detuning parameter—in close agreement with the steady-state predictions of Kuizenga and Siegman [23]. More importantly, they found that perturbations to the steady-state laser pulse grow and "drift" through the pulse with a constant velocity. As the detuning is increased, their findings suggest that no stable pulse can be maintained as perturbations can grow large enough to compete with the existing laser pulse. This results in a destabilizing of the laser which they identify as a drift instability.

More recently, Kärtner, Zumbühl, and Matuschek [21] suggested that this instability exhibits a transition to turbulence. They showed that the detuned laser is an example of a nonnormal system and, as a result, perturbations to the ground-mode pulse are subject to strong transient growth analogous to that experienced by the laminar state in fluid pipe flow [38]. Furthermore, they quantified the effect of detuning and predicted that the transient growth scales with the exponential of the detuning parameter. The precise nature of the instability was not considered, however; nor was the connection to the drift velocity of Morgner and Mitschke.

Similar results have been predicted for the frequency-modulated laser by Longhi and Laporta [26]. In addition to showing that perturbations are subject to large transient amplification due to the nonorthogonality of the laser modes, they also showed that the laser exhibits a strongly enhanced sensitivity to external noise. The existence of so-called excess noise was first predicted by Petermann [30] in 1979 in the context of a gain-guided laser amplifier but has since been generalized to a wide array of optical systems, including general nonorthogonal optical systems [34, 35] and even nonorthogonal polarization modes [39]. As a result, the response of any laser system to noise is often characterized by the Petermann excess noise factor.

The purpose of this paper is to conduct a careful investigation of the dynamics of pulse formation in an amplitude-modulated laser. We show that the transient growth expected at the lasing threshold is equivalent to the Petermann excess noise factor, and we find exact expressions for the transient growth factor away from threshold. Moreover, we find an exact reduction from the governing PDEs to a low-dimensional system of ODEs for the parameters of a circulating pulse. We show that the evolving ground-mode pulse is a globally attracting solution of this system. In the presence of noise, however, we demonstrate numerically that the laser destabilizes and undergoes a repeating cycle of pulse creation and annihilation.

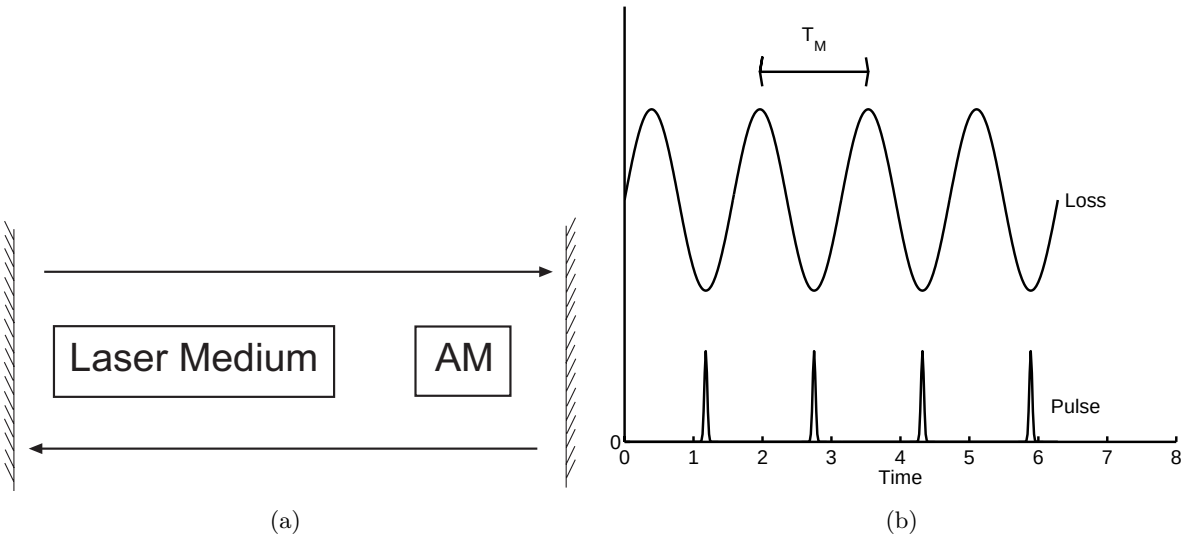

Figure 2.1. (a) *An actively mode-locked laser consisting of an optical resonator, a laser medium, and an amplitude modulator.* (b) *Laser pulses can form only when the losses are minimum.*

2. Governing equations. A schematic of an actively mode-locked laser is shown in Figure 2.1. An amplitude modulator is placed inside a laser cavity, with a modulation period T_M that closely matches the round-trip time T_R of the laser cavity. As a result of the losses introduced by the modulator, the laser pulses are expected to have a pulse-width much shorter than the round-trip time of the cavity, which allows us to describe the laser on two independent time scales. The cavity time T is sampled on the cavity round-trip time T_R, which is typically on the order of nano-seconds. In contrast, the local time t resolves the resulting pulse shape, which may be on the order of pico-seconds. The evolution equations for the complex electric field envelope $A(T,t)$ and the laser gain $g(T)$ for $t \in (-\infty,\infty)$ and $T \in [0,\infty)$ are [21, 10]

$$T_R \frac{\partial A(T,t)}{\partial T} = \left(g(T) - l - \mu t^2\right) A(T,t) + \Gamma \frac{\partial A(T,t)}{\partial t} + D\frac{\partial^2 A(T,t)}{\partial t^2}\ , \tag{2.1}$$

$$\frac{dg(T)}{dT} = \alpha - \gamma g(T) - \beta g(T)||A(T,*)||^2\ , \tag{2.2}$$

where the pulse energy, $||A(T,*)||^2$, is defined in terms of the standard inner-product on $L^2(-\infty,\infty)$, i.e.,

$$||A(T,*)||^2 = \langle A(T,*), A(T,*)\rangle = \int_{-\infty}^{\infty} |A(T,t)|^2 dt.$$

The evolution equation (2.1) for the pulse envelope includes a number of relevant physical effects. The pulse experiences both gain, $g(T)$, and loss, $D\partial_{tt} - l - \mu t^2$, as it propagates in the cavity. The parameter l represents the fixed cavity losses which are frequency-independent, while D represents the curvature of the intracavity losses in the frequency domain which limits the bandwidth of the laser. The parameter μ is proportional to the depth of the loss modulation. While the losses are actually modulated periodically, the modulation depth is relatively large so that radiation can only build up during the time of low intracavity loss, which is much shorter than the modulator period. In that case, the cosine modulation is approximated by a parabola so that μ actually represents the curvature of the loss modulation at the point of minimum loss. In addition, the loss modulation period is not perfectly matched to the round-trip time and this detuning is captured by $\Gamma = T_M - T_R$.

The dynamics of the gain medium is captured in (2.2). The gain in the cavity, $g(T)$, depends on the amount of energy driving the laser, the rate at which the gain medium can radiate the laser photons, and the number of photons present in the cavity. The parameter α accounts for the rate of energy gain due to pumping, γ represents the gain relaxation rate, and β is related to the saturation power of the gain medium. The number of photons in the cavity at any given time T is proportional to the pulse energy, $||A(T,*)||^2$.

The evolution equations, (2.1) and (2.2), are of course supplemented with both initial, $A(T=0,t)$ and $g(T=0)$, and boundary conditions. Our search for pulse-like solutions requires us to satisfy vanishing or Dirichlet boundary conditions for the pulse amplitude, i.e.,

$$\lim_{t\to\pm\infty} A(T,t) = 0. \tag{2.3}$$

Finally, there are several restrictions on the parameters, all of which are assumed real in this paper. Γ may be positive or negative, while l, μ, D, α, γ, and β are all positive. For

the purpose of the simulations presented in this paper, the following fixed values were used: $l = 0.01$, $\mu = 1$, $D = 0.0001$, $\gamma = 0.01$, $\beta = 0.1$, and $T_R = 1$. The parameters Γ and α were varied as needed.

3. Steady-state solutions. The steady-state solutions of (2.1)–(2.2) are defined when both $A(T,t) = A_s(t)$ and $g(T) = g_s$ are independent of T, i.e.,

$$\left(g_s - l - \mu t^2 + \Gamma\partial_t + D\partial_{tt}\right) A_s = 0, \tag{3.1}$$

$$\alpha - \gamma g_s - \beta g_s ||A_s||^2 = 0. \tag{3.2}$$

A cursory inspection of (3.1)–(3.2) reveals that there is a trivial steady-state solution, $A_s = 0$ and $g_s = \alpha/\gamma$. This corresponds to the laser being "off." There are, of course, steady-state solutions which correspond to the laser being on and *mode-locked* and which can be found by looking for nontrivial solutions to (3.1) subject to the boundary conditions (2.3). These nontrivial solutions can be determined by looking for a solution of the form

$$A_s(t) = \psi(t) \exp\left(-\frac{(t-a)^2}{2\sigma^2}\right), \tag{3.3}$$

where a and σ are free parameters to be determined. Substituting ansatz (3.3) into (3.1) results in

$$\begin{aligned} &D\psi_{tt} + \left(\frac{\Gamma\sigma^2 - 2D(t-a)}{\sigma^2}\right)\psi_t \\ &\quad + \left(g_s - l - \mu t^2 + \frac{D(t-a)^2 - D\sigma^2 - \Gamma\sigma^2(t-a)}{\sigma^4}\right)\psi = 0\,. \end{aligned} \tag{3.4}$$

This equation can be transformed into the Hermite equation by a judicious choice of a and σ. If we define

$$\sigma^2 = \sqrt{D/\mu}, \tag{3.5}$$

$$a = -\sigma^2\Gamma/2D \tag{3.6}$$

and transform the variable t by $t \to \sigma u$, the resulting equation is

$$\psi_{uu} - 2u\psi_u + \frac{1}{\sqrt{\mu D}}\left(g_s - l - \sqrt{\mu D} - \frac{\Gamma^2}{4D}\right)\psi = 0\,. \tag{3.7}$$

This is precisely the Hermite equation if

$$\frac{1}{\sqrt{\mu D}}\left(g_s - l - \sqrt{\mu D} - \frac{\Gamma^2}{4D}\right) = 2n; \quad n = 0, 1, 2, \ldots\,, \tag{3.8}$$

which must be true in order to satisfy the boundary conditions (2.3). In other words, a nontrivial solution exists for the pulse amplitude $\psi(t)$ if the steady-state gain, $g_s = g_n$, is given by

$$g_n = l + \left(2\sqrt{\mu D}\left(\Delta^2 + n + \frac{1}{2}\right)\right), \quad n = 0, 1, 2, \ldots\,, \tag{3.9}$$

where Δ is a normalized detuning, $\Delta = \sigma\Gamma/\sqrt{8}D$. If this is the case, then (3.7) is the Hermite equation with the usual Hermite polynomials $H_n(u)$ as solutions. Each value of n in (3.9) gives us a steady-state pulse $A_s(t) = A_n(t)$, which is a Hermite–Gaussian mode of the form

$$A_n(t) = K_n\, H_n\left(\frac{t}{\sigma}\right) \exp\left(-\frac{(t-a)^2}{2\sigma^2}\right). \tag{3.10}$$

The pulse amplitudes, K_n, are determined via (3.2), which gives

$$||A_n||^2 = \frac{\alpha\ -\gamma\ g_n}{\beta g_n}. \tag{3.11}$$

Since the sequence g_n increases linearly with n, the threshold for lasing operation is given by $\alpha = \alpha_{th} = \gamma\ g_0$, as this is the first value of α which permits the existence of a pulse. We expect the ground-mode ($n = 0$) to dominate, at least close to the lasing threshold. The basic lasing solution is a Hermite–Gaussian pulse of width σ centered at $t = a = -\sqrt{2}\sigma\Delta$. If the modulator period matches the round-trip period perfectly, i.e., $\Delta = 0$, then the pulse is centered at $t = 0$, which corresponds to the minimum loss point. If, on the other hand, there is any slight detuning, i.e., $\Delta \neq 0$, then the pulse will be shifted away from the minimum loss point by an amount proportional to the detuning.

4. Linear stability analysis. Haus [19] demonstrated that the trivial solution loses stability to the ground-mode at $\alpha = \alpha_{th} = \gamma g_0$, and to the nth-order mode when $\alpha = \gamma g_n$. He also showed that the ground-mode is linearly stable to the higher-order modes and that the higher-order modes are linearly unstable to the lower-order modes. As mentioned earlier, we would therefore expect that, close to threshold, the ground-mode will be favored.

These linear stability results are limited, however, for reasons that will be detailed in the following section on transient growth. Both for completeness and as a means of motivating this work, we include here a detailed linear stability analysis. Linearization of the governing equations, (2.1) and (2.2), about one of the steady-state solutions ($A = A_s$, $g = g_s$) leads to

$$T_R\frac{\partial}{\partial T}A(T,t) = \left(g_s - l - \mu t^2 + \Gamma\partial_t + D\partial_{tt}\right)A(T,t) + g(T)A_s(t), \tag{4.1}$$

$$\frac{d}{dT}g(T) = -\frac{\alpha}{g_s}g(T) - \beta g_s\left(\langle A_s, A\rangle + \langle A, A_s\rangle\right), \tag{4.2}$$

where $A(T,t)$ and $g(T)$ now represent perturbations to the steady-state solution.

4.1. Trivial steady-state. We begin by considering the stability of the trivial solution, $A_s = 0$ and $g_s = \alpha/\gamma$. In this case the linearized equations reduce to

$$T_R\frac{\partial}{\partial T}A(T,t) = \left(\frac{\alpha}{\gamma} - l - \mu t^2 + \Gamma\partial_t + D\partial_{tt}\right)A(T,t), \tag{4.3}$$

$$\frac{d}{dT}g(T) = -\gamma g(T). \tag{4.4}$$

Note that the pulse envelope and the gain are now decoupled. Perturbations to the gain clearly decay to zero on a time scale of $1/\gamma$. Turning to the pulse envelope equation, the

eigenvalues, λ_n, and eigenfunctions, $\phi_n(t)$, of (4.3) subject to the boundary conditions (2.3) follow naturally from the steady-state solutions (3.10), and we have

$$\left(\frac{\alpha}{\gamma} - l - \mu t^2 + \Gamma\partial_t + D\partial_{tt}\right)\phi_n(t) = \lambda_n\phi_n(t), \tag{4.5}$$

$$\lambda_n = \frac{\alpha}{\gamma} - g_n, \quad n = 0, 1, 2, \dots, \tag{4.6}$$

$$\phi_n(t) = H_n\left(\frac{t}{\sigma}\right)\exp\left(-\frac{(t-a)^2}{2\sigma^2}\right). \tag{4.7}$$

Recalling the nature of g_n, (3.9), reveals that as the pumping parameter α is increased the trivial solution first loses stability to the $n = 0$ mode at $\alpha_{th} = \gamma g_0$. Increasing α further will result in the trivial solution also losing stability to the $n = 1$ mode at $\alpha = \gamma g_1$, the $n = 2$ mode at $\alpha = \gamma g_2$, and so forth.

4.2. Nontrivial steady-state. Linearizing the governing equations about one of the nontrivial solutions, $A = A_n$ and $g = g_n$, leads to the set of equations

$$T_R\frac{\partial}{\partial T}A(T,t) = \left(g_n - l - \mu t^2 + \Gamma\partial_t + D\partial_{tt}\right)A(T,t) + g(T)A_n(t), \tag{4.8}$$

$$\frac{d}{dT}g(T) = -\frac{\alpha}{g_n}g(T) - \beta g_n\left(\langle A_n, A\rangle + \langle A, A_n\rangle\right), \tag{4.9}$$

where $A(T,t)$ and $g(T)$ represent perturbations to the nontrivial solution.

We now seek a solution for $A(T,t)$ in the form of a time-dependent linear combination of the first $N+1$ Hermite–Gaussian modes,

$$A(T,t) = \sum_{j=0}^{N} C_j(T)H_j\left(\frac{t}{\sigma}\right)\exp\left(-\frac{(t-a)^2}{2\sigma^2}\right), \tag{4.10}$$

where a and σ take the values shown in (3.5) and (3.6). If we substitute (4.10) into (4.8) and (4.9) and use the recursive properties of the Hermite polynomials and the linear independence of the Hermite–Gaussians, we arrive at the set of linear ODEs

$$T_R\frac{d}{dT}C_n(T) = K_n g(T), \tag{4.11}$$

$$T_R\frac{d}{dT}C_j(T) = (g_n - g_j)C_j(T), \quad j = 0, 1, 2, \dots, N, \quad j \neq n, \tag{4.12}$$

$$\frac{d}{dT}g(T) = -\frac{\alpha}{g_n}g(T) - 2\beta g_n K_n\sum_{j=0}^{N} M_{nj}C_j(T), \tag{4.13}$$

where the interaction matrix elements, M_{nj}, are given by

$$M_{nj} = \int_{-\infty}^{\infty} H_n\left(\frac{t}{\sigma}\right)H_j\left(\frac{t}{\sigma}\right)\exp\left(-\frac{(t-a)^2}{\sigma^2}\right)dt.$$

Let us first consider the stability of the ground-mode, $n = 0$. The eigenvalues, $\{\lambda_j\}_{j=1}^{N+2}$, of this system of $N + 2$ linear differential equations can be determined explicitly and are

$$\lambda_1 = -\frac{\alpha T_R}{2g_0}\left(1 + \sqrt{1 - \frac{8(\alpha - \gamma g_0)g_0^2}{\alpha^2 T_R}}\right), \tag{4.14}$$

$$\lambda_2 = -\frac{\alpha T_R}{2g_0}\left(1 - \sqrt{1 - \frac{8(\alpha - \gamma g_0)g_0^2}{\alpha^2 T_R}}\right), \tag{4.15}$$

$$\lambda_j = g_0 - g_{j-2}, \quad j = 3, 4, \ldots, N + 2. \tag{4.16}$$

The first two eigenvalues involve the coupling between perturbations to the ground-mode and to the gain. Recalling that $\alpha - \gamma g_0 > 0$ for the ground-mode to exist implies that these perturbations are always damped since both eigenvalues have negative real parts. The third eigenvalue governs the dynamics of perturbations along the $n = 1$ mode and the coupling between it, the ground-mode, and the gain. These perturbations are always damped since $g_1 > g_0$. The other eigenvalues follow suit, and perturbations along the higher-order modes are more heavily damped. We therefore conclude that the ground-mode is linearly stable to arbitrary perturbations. If we consider the stability of the higher-order modes, $n > 0$, then (4.12) shows that these modes are always unstable to each of the lower-order modes.

In summary, then, we have confirmed that if $\alpha < \alpha_{th}$, the trivial solution is linearly stable. If, on the other hand, $\alpha > \alpha_{th}$, the trivial solution is linearly unstable, and the $n = 0$ mode begins to grow. The other modes also turn on as α is further increased. The $n = 0$ mode is linearly stable to arbitrary perturbations if $\alpha > \alpha_{th}$, and the higher-order modes are linearly unstable to the $n = 0$ mode. Linear analysis suggests, therefore, that below threshold the laser will remain "off," while above threshold the laser will "turn on" and form a mode-locked pulse.

5. Transient growth. Linear stability theory guarantees only that infinitesimal perturbations will die off asymptotically; short-term growth is a possibility. If the linear operator is *normal* [1, 28], then this can be strengthened further and we can conclude that perturbations cannot grow. On the other hand, nonnormal operators allow for short-term transient growth of perturbations.

The importance of nonnormal operators emerged recently in the context of viscous shear flow [11, 31, 32, 38] as a possible mechanism for the instability of the laminar flow below threshold. The nonorthogonality of the eigenfunctions of the linear operator results in short-term transient growth of perturbations to the laminar state. The subsequent interplay between transient growth and nonlinear mixing may be enough to then destabilize the system. The calculation of the magnitude of transient growth expected [31] and of the types of perturbations which experience maximum transient growth [11] is complicated by the nature of the linear operator.

In the context of actively mode-locked lasers, Kärtner, Zumbühl, and Matuschek [21] pointed out that the linearized amplitude-modulated laser is governed by a nonnormal operator. They suggested that the degree of nonnormality depends strongly on the detuning Δ and

that transient growth on the order of $\exp(4\Delta^2)$ could be expected. Longhi and Laporta [26] have reported similar findings for the frequency-modulated laser.

The relevance of nonnormal operators to laser systems is much older, however, than the dates of these studies might suggest. It has been known since the seminal work of Petermann in 1979 that, in the presence of stochastic forcing, laser systems governed by nonnormal operators are subject to excess noise [30, 34, 35]. (Laser operation depends on the presence of such stochastic forcing in the form of spontaneous emission noise.) The Petermann excess noise factor (K) is a measure of the enhancement of the noise source and is given by

$$K = \frac{\langle u, u\rangle \, \langle v, v\rangle}{\langle u, v\rangle^2}, \tag{5.1}$$

where u is the eigenfunction of the linear operator, v is the adjoint eigenfunction, and $\langle *, *\rangle$ is an appropriate inner-product.

We will show in section 5.1 that the growth sustained by perturbations at the lasing threshold is precisely the Petermann excess noise factor. Furthermore, it will become clear that the perturbation which leads to maximum growth is the adjoint eigenmode, in agreement with known results in viscous shear flow [11]. Below threshold we compute the optimal growth curve [32, 38] by evaluating the norm of the solution operator to the linearized equation; the solution operator is based on the truncated Hermite expansion discussed in [2]. We find that the transient growth below threshold is bounded in magnitude by $\exp(4\Delta^2)$ and that the perturbation which experiences most growth is closely related to the adjoint mode. In section 6 we confirm these numerical results by finding explicit analytical expressions for the transient growth below threshold as well as the form of the relevant perturbation. In section 5.2 we compute the optimal growth curve for the linear operator above threshold and find again that the growth is bounded by $\exp(4\Delta^2)$. The perturbation which gives rise to the maximum transient growth in this case is the adjoint mode.

5.1. Below threshold. In light of this, let us reconsider the linear stability of the nonlasing solution. Recall that the nonlasing solution is defined by $A_s = 0$ and $g_s = \alpha/\gamma$. The linearized equations, already introduced in section 4, are

$$T_R \frac{\partial}{\partial T} A(T,t) = \mathcal{L} A(T,t), \tag{5.2}$$

$$\frac{d}{dT} g(T) = -\gamma g(T), \tag{5.3}$$

$$\mathcal{L} = \frac{\alpha}{\gamma} - l - \mu t^2 + \Gamma \partial_t + D \partial_{tt}, \tag{5.4}$$

where again $g(T)$ and $A(T,t)$ represent perturbations to the nonlasing solution. We have already determined the eigenvalues, λ_n, and eigenfunctions, $\phi_n(t)$, of $\mathcal{L}$ subject to boundary conditions (2.3),

$$\mathcal{L}\phi_n(t) = \lambda_n \phi_n(t), \tag{5.5}$$

$$\lambda_n = \frac{\alpha}{\gamma} - g_n, \quad n = 0, 1, \dots, \tag{5.6}$$

$$\phi_n(t) = H_n\left(\frac{t}{\sigma}\right) \exp\left(-\frac{(t-a)^2}{2\sigma^2}\right). \tag{5.7}$$

We will also require the adjoint modes. The adjoint operator, defined as usual by

$$\langle u, \mathcal{L}v\rangle = \langle \mathcal{L}^* u, v\rangle, \tag{5.8}$$

is given by

$$\mathcal{L}^* = \frac{\alpha}{\gamma} - l - \mu t^2 - \Gamma\partial_t + D\partial_{tt}. \tag{5.9}$$

The adjoint operator $\mathcal{L}^*$ can be obtained from $\mathcal{L}$ by making the transformation $\Gamma \to -\Gamma$. The eigenvalues μ_n and eigenfunctions ψ_n of $\mathcal{L}^*$ subject to the boundary conditions (2.3) are given by

$$\mathcal{L}^*\psi_n(t) = \mu_n\psi_n(t), \tag{5.10}$$

$$\mu_n = \frac{\alpha}{\gamma} - g_n, \quad n = 0, 1, \dots, \tag{5.11}$$

$$\psi_n(t) = H_n\left(\frac{t}{\sigma}\right)\exp\left(-\frac{(t+a)^2}{2\sigma^2}\right). \tag{5.12}$$

The dependence of g_n on Γ^2 leaves the eigenvalues unchanged under the transformation, and the linear dependence of a on Γ means that the adjoint modes are the Hermite–Gaussians with the Gaussian centered at $t = -a$.

The general solution to (5.2) is given by

$$A(T,t) = \sum_{n=0}^{\infty} a_n\phi_n(t)e^{\lambda_n T/T_R},$$

where the a_n's are chosen to satisfy the initial condition

$$A(0,t) = \sum_{n=0}^{\infty} a_n\phi_n(t).$$

Recalling that the eigenfunctions and their adjoints form a biorthogonal set [28, 33], we can determine the coefficients a_n by projecting onto the adjoint to give

$$a_n = \frac{\langle A(0,t), \psi_n(t)\rangle}{\langle \phi_n(t), \psi_n(t)\rangle},$$

where $\langle *, *\rangle$ is again the standard inner-product on $L^2(-\infty, \infty)$. The general solution to the linearized problem is then

$$A(T,t) = \sum_{n=0}^{\infty} \frac{\langle A(0,t), \psi_n(t)\rangle}{\langle \phi_n(t), \psi_n(t)\rangle}\ \phi_n(t)\ e^{\lambda_n T/T_R}.$$

Below the lasing threshold, all of the eigenvalues are negative. As we approach threshold, however, the leading eigenvalue approaches zero. Let us first consider the perturbation dynamics at threshold. Since $\lambda_0 = 0$ and $\dots \lambda_3 < \lambda_2 < \lambda_1 < 0$, in the limit as $T \to \infty$ we find that

$$A_\infty(t) = \lim_{T\to\infty} A(T,t) = \frac{\langle A(0,t), \psi_0(t)\rangle}{\langle \phi_0(t), \psi_0(t)\rangle}\ \phi_0(t)$$

so that the dynamics eventually collapse onto the ground-mode as we would expect since the ground-mode is neutrally stable at threshold and all other modes are unstable. The energy of this solution is then

$$||A_\infty(t)||^2 = \langle A_\infty(t), A_\infty(t)\rangle = \frac{\langle A(0,t),\psi_0(t)\rangle^2\langle\phi_0(t),\phi_0(t)\rangle}{\langle\phi_0(t),\psi_0(t)\rangle^2}.$$

For a given ground-state mode this depends only on the initial condition, and the energy is maximized if the initial condition is parallel to the adjoint ground-mode, i.e.,

$$A(0,t) \propto \psi_0(t). \tag{5.13}$$

In this case the energy growth factor is

$$\text{Growth} = \frac{||A_\infty(t)||^2}{||A(0,t)||^2} = \frac{\langle\phi_0(t),\phi_0(t)\rangle\langle\psi_0(t),\psi_0(t)\rangle}{\langle\phi_0(t),\psi_0(t)\rangle^2}, \tag{5.14}$$

which is precisely the Petermann excess noise factor of (5.1). The inner-products are given by

$$\begin{aligned}
\langle\phi_0(t),\phi_0(t)\rangle &= \int_{-\infty}^{\infty} \exp\left(-\frac{(t-a)^2}{\sigma^2}\right) dt = \sigma\sqrt{\pi},\\
\langle\psi_0(t),\psi_0(t)\rangle &= \int_{-\infty}^{\infty} \exp\left(-\frac{(t+a)^2}{\sigma^2}\right) dt = \sigma\sqrt{\pi},\\
\langle\phi_0(t),\psi_0(t)\rangle &= \int_{-\infty}^{\infty} \exp\left(-\frac{(t-a)^2}{2\sigma^2}\right)\exp\left(-\frac{(t+a)^2}{2\sigma^2}\right) dt,\\
&= \exp\left(-\frac{a^2}{\sigma^2}\right)\int_{-\infty}^{\infty}\exp\left(-\frac{t^2}{\sigma^2}\right) dt,\\
&= \sigma\sqrt{\pi}\exp\left(-\frac{a^2}{\sigma^2}\right),
\end{aligned}$$

and the energy growth is then

$$\text{Growth} = \exp\left(\frac{2a^2}{\sigma^2}\right) = \exp\left(4\Delta^2\right),$$

which agrees with the results of Kärtner, Zumbühl, and Matuschek [21].

We have shown that if we linearize the governing equations about the trivial solution, then the resulting linear system can be solved exactly. Since the leading eigenvalue is zero at threshold, any perturbation eventually collapses onto the ground-mode, which is a Gaussian pulse located at $t = a$. If we ask which perturbation leads to the most growth in energy, it is the adjoint ground-mode, which corresponds to a Gaussian pulse located at $t = -a$. We show in section 6 how such a perturbation evolves into the ground-mode, but in any case the linear growth experienced by such a perturbation has an exponential dependence on Δ^2.

Below threshold, we compute the optimal growth curve in order to identify the optimal perturbation which leads to maximum transient growth [32, 38]. The optimal growth energy is defined as the norm of the solution operator to (5.2), i.e., $||\exp(\mathcal{L}t/T_R)||^2$, where $\mathcal{L}$ is defined

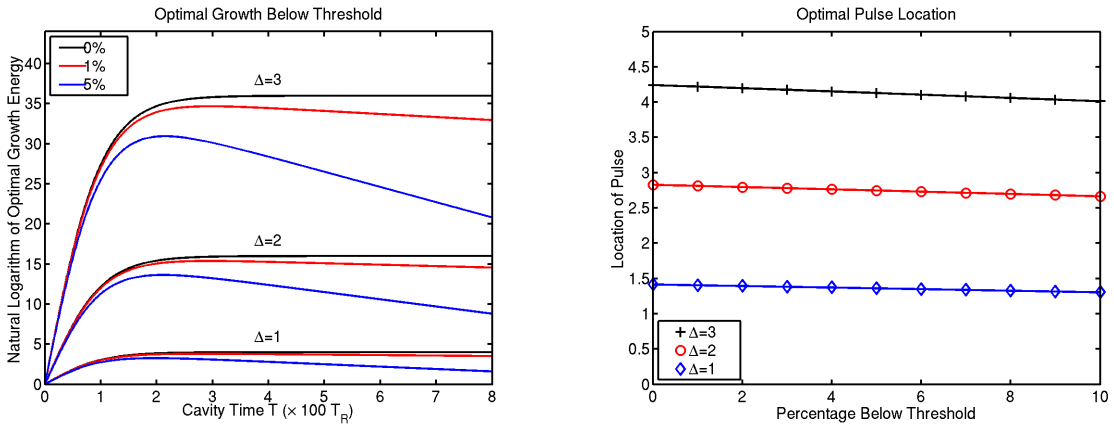

(a) (b)

Figure 5.1. (a) *Optimal growth curves below threshold for various values of* α *and* Δ. (b) *Location of optimum pulse.*

in (5.4). Our algorithm is based on a spectral Hermite approximation, as discussed in [2]. In each computation discussed below we use 128 basis functions. We vary α and Δ and set all other parameters to the values given in section 2.

In Figure 5.1(a) we show the natural logarithm of the optimal growth energy against cavity time T for different values of Δ and α. For each value of Δ we vary α from its threshold value to 5% below threshold. (Recall that α_{th} depends on Δ.) At threshold, the optimal growth energy increases exponentially before leveling off at the expected value of $\exp(4\Delta^2)$. Below threshold, the optimal growth energy increases exponentially, reaches a maximum value, and then decays exponentially. While the maximum energy obtained in each case is less than that obtained at threshold, it is still of the same order. In addition, the time taken to reach maximum energy depends on Δ and decreases as we move below threshold. The precise relationship between α, Δ, the maximum energy, and the time taken to reach maximum energy can be obtained exactly and is discussed in section 6.

The optimal perturbation which leads to maximum transient growth is determined by first finding the time of maximum growth and then computing the SVD of the matrix exponential; the leading singular vector gives the optimal perturbation [32, 38]. We find numerically that the optimal perturbation is a single Gaussian pulse of equilibrium width. In Figure 5.1(b) we graph the optimal pulse location determined numerically (symbols) and the exact optimal location (solid lines) obtained in section 6. These results demonstrate that at threshold the pulse occupies the adjoint location as expected. Below threshold, however, the optimal pulse location moves toward the origin.

The transient pulse formation dynamics are captured in Figure 5.2, which shows a contour plot of the pulse amplitude as a function of local time t and cavity time T for $\Delta = 1$ at 5% below threshold. An initial optimum pulse grows exponentially as it sweeps across the domain into position. The time taken to attain maximum energy roughly coincides with the time taken to sweep into position. After this point, the pulse-amplitude decays exponentially to zero. In section 6, we will find an explicit solution for the pulse-location and pulse-amplitude as a

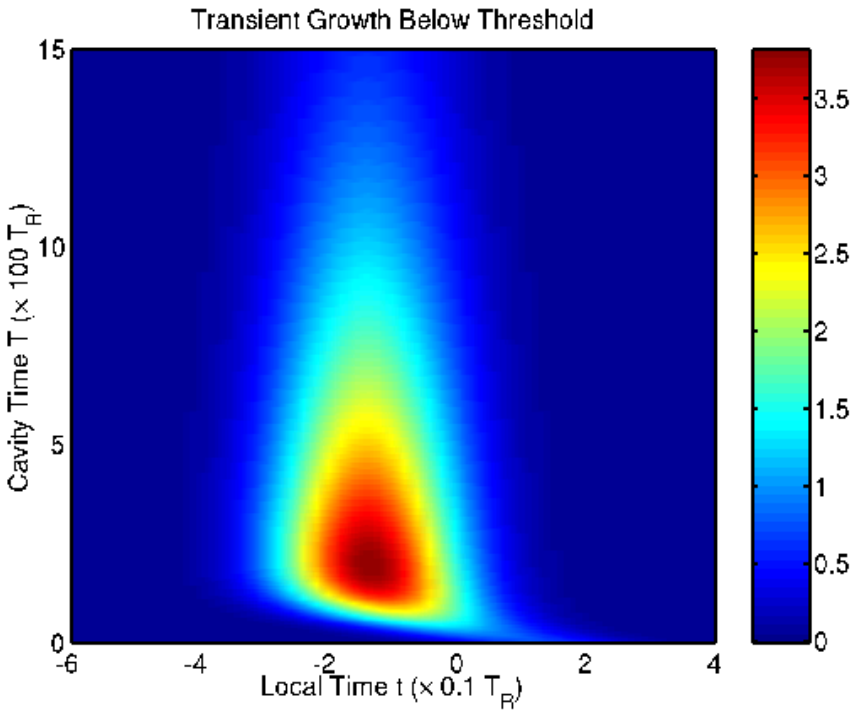

Figure 5.2. *Contour plot of pulse-amplitude versus local time t and cavity time T for $\Delta = 1$ at 5% below threshold. The initial condition corresponds to an optimum pulse centered at $t = \sqrt{1.85} \times 0.1 T_R$.*

function of T which will confirm these numerical experiments.

5.2. Above threshold. Above threshold, the growth of an optimal perturbation to the trivial solution is no longer transient since the trivial solution itself becomes unstable to the ground-mode pulse. In this regime, we need to consider the equations linearized about the ground-mode, A_0 and g_0. In this case they are

$$T_R \frac{\partial}{\partial T} A(T,t) = \left(g_0 - l - \mu t^2 + \Gamma \partial_t + D\partial_{tt}\right) A(T,t) + g(T) A_0(t), \tag{5.15}$$

$$\frac{d}{dT} g(T) = -\frac{\alpha}{g_0} g(T) - \beta g_0 \left(\langle A_0, A\rangle + \langle A, A_0\rangle\right), \tag{5.16}$$

where $A(T,t)$ and $g(T)$ represent perturbations to the ground-mode solution.

In Figure 5.3(a) we show the optimal growth results for several different values of Δ with α held at 5% above threshold. In each case, we compute the norm of the solution operator to the linearized equations, (5.15) and (5.16). Above threshold, the optimal energy initially grows exponentially before dying off. The nature of the die-off changes as we increase Δ since the leading eigenvalue becomes complex. The oscillation period matches that predicted by linear stability analysis. In Figure 5.3(b) we set $\Delta = 3$ and show the results as we change α from its threshold value to 5% above threshold. At threshold, the linear operator governing perturbations to an equilibrium ground-mode pulse matches the linear operator which governs perturbations to the trivial solution. The growth at threshold should therefore be $\exp(4\Delta^2)$,

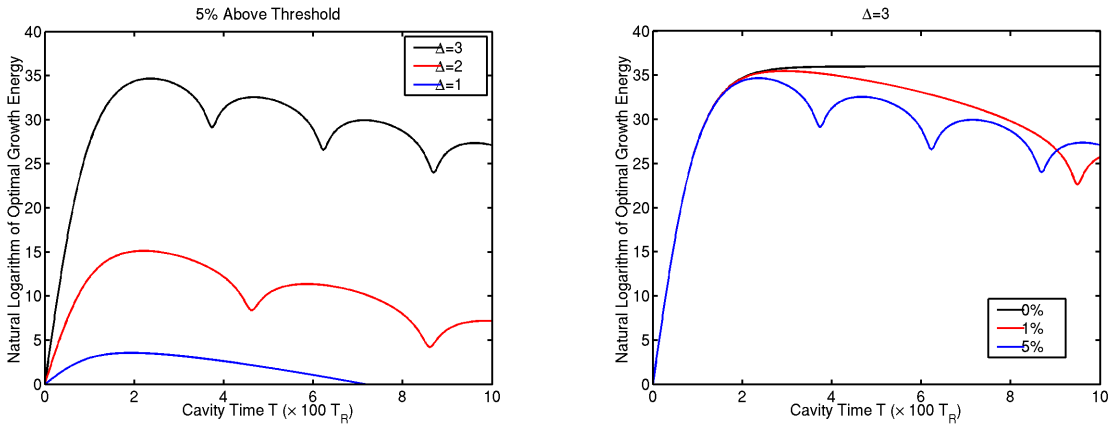

Figure 5.3. *Optimal growth curves above threshold:* (a) *Natural logarithm of optimal growth energy versus cavity time as a function of* Δ *at* 5% *above threshold;* (b) *natural logarithm of optimal growth energy versus cavity time as a function of* α *for* $\Delta = 3$.

and this is indeed the case. The growth above threshold is bounded by this value, and computing the SVD of the matrix exponential at the time of maximum energy reveals that the adjoint mode is in fact the optimal perturbation. We have checked this result for various values of Δ and up to 50% above threshold.

6. Nonlinear dynamics.

The linear stability analysis of section 4 and the details on transient growth of section 5 provide us with a general picture of the linear dynamics of perturbations to both the trivial solution and the ground-mode pulse. We now consider the full nonlinear dynamics of pulse formation. We begin by considering the evolution of a single pulse, for which an exact reduction to a low-dimensional system of nonlinear ODEs is available—the so-called pulse-parameter equations. We use a linearized version of these equations to extend our results on transient growth, and we show analytically that above threshold a ground-mode pulse is an attracting fixed point of the nonlinear system. These results are confirmed by direct simulation of the ODEs using an implicit method [2].

We conclude this section with a series of full simulations of the governing PDEs in the presence of noise. In the first set of simulations, we consider the interaction between a ground-mode pulse and a single noise pulse. In concert with our transient growth predictions, we find that a ground-mode pulse undergoes a strong interaction with a noise pulse but that a ground-mode pulse eventually re-emerges from this interaction. In the second and final set of simulations, we include a stochastic noise source and find that the ground-mode pulse repeatedly undergoes a process of creation and annihilation which could be interpreted as turbulent dynamics [21].

6.1. Single pulse evolution.

In this section we address the question of how a single ground-mode pulse evolves from the trivial solution. A reduction to a set of pulse-parameter equations is achieved by seeking a ground-mode pulse whose pulse parameters depend on T. This is motivated by the steady-state circulating Gaussian pulse analysis work of Kuizenga

and Seigman [23], but we derive dynamic pulse-parameter equations in a systematic manner.

We first assume a pulse solution of the form

$$A(T,t) = \psi(T)\exp\left(-\frac{(t-a(T))^2}{2\sigma^2(T)}\right), \tag{6.1}$$

where the pulse parameters $\psi(T)$, $a(T)$, and $\sigma(T)$ represent the pulse-amplitude, pulse-location, and pulse-width, respectively. In light of our choice of real parameters, we may choose the pulse parameters to be real without loss of generality. The following derivatives are required:

$$\begin{aligned}
\Gamma\frac{\partial A}{\partial t} &= -\frac{\Gamma\psi(t-a)}{\sigma^2}\exp\left(-\frac{(t-a)^2}{2\sigma^2}\right),\\
D\frac{\partial^2 A}{\partial t^2} &= \left(-\frac{D\psi}{\sigma^2}+\frac{D\psi(t-a)^2}{\sigma^4}\right)\exp\left(-\frac{(t-a)^2}{2\sigma^2}\right),\\
T_R\frac{\partial A}{\partial T} &= \left(T_R\psi_T+\frac{T_R\psi a_T(t-a)}{\sigma^2}+\frac{T_R\psi(\sigma^2)_T(t-a)^2}{2\sigma^4}\right)\exp\left(-\frac{(t-a)^2}{2\sigma^2}\right),
\end{aligned}$$

and we write $\mu t^2 = \mu(t-a)^2 + 2a\mu(t-a) + \mu a^2$. Substituting these derivatives into the governing equation (2.1) and grouping terms into the form of standard polynomials give

$$\begin{aligned}
&T_R\left(\psi_T P_0(u)+\frac{a_T}{\sigma}\psi P_1(u)+\frac{\sigma_T}{\sigma}\psi P_2(u)\right)\exp\left(-\frac{u^2}{2}\right)\\
&=\left(g-l-\mu a^2-\frac{D}{\sigma^2}\right)\psi P_0(u)\exp\left(-\frac{u^2}{2}\right)\\
&-\left(2\mu\sigma a+\frac{\Gamma}{\sigma}\right)\psi P_1(u)\exp\left(-\frac{u^2}{2}\right)\\
&+\left(\frac{D}{\sigma^2}-\mu\sigma^2\right)\psi P_2(u)\exp\left(-\frac{u^2}{2}\right),
\end{aligned}$$

where $u=(t-a)/\sigma$ and $P_j(u)=u^j$. Linear independence of the polynomials $P_j(u)$ leads to the following set of differential equations for the pulse-parameters:

$$\begin{aligned}
T_R\frac{d}{dT}\sigma^2 &= 2(D-\mu\sigma^4),\\
T_R\frac{d}{dT}a &= -\Gamma-2\mu\sigma^2 a,\\
T_R\frac{d}{dT}\psi &= \left(g-l-\mu a^2-\frac{D}{\sigma^2}\right)\psi.
\end{aligned}$$

Turning our attention to the gain equation, (2.2), the pulse ansatz (6.1) leads to

$$\begin{aligned}
\frac{d}{dT}g &= \alpha-\gamma g-\beta g\psi^2\int_{-\infty}^{\infty}\exp\left(-\frac{(t-a)^2}{\sigma^2}\right)dt\\
&= \alpha-\gamma g-\beta g\psi^2\sigma\sqrt{\pi}.
\end{aligned}$$

The pulse-parameter equations are then

$$T_R \frac{d}{dT}\sigma^2 = 2(D - \mu\sigma^4), \tag{6.2}$$

$$T_R \frac{d}{dT}a = -\Gamma - 2\mu\sigma^2 a, \tag{6.3}$$

$$T_R \frac{d}{dT}\psi = \left(g - l - \mu a^2 - \frac{D}{\sigma^2}\right)\psi, \tag{6.4}$$

$$\frac{d}{dT}g = \alpha - \gamma g - \sqrt{\pi}\beta\sigma g\psi^2. \tag{6.5}$$

The system of equations (6.2)–(6.5) forms a hierarchy in the following sense. The pulse-width, $\sigma(T)$, evolves independently of the other pulse-parameters. The pulse-location, $a(T)$, is driven by the dynamics of the pulse-width. The pulse-amplitude, $\psi(T)$, and gain, $g(T)$, are mutually coupled and depend on the pulse-width and pulse-position. There are two fixed points of this dynamical system. In both cases, the equilibrium pulse-width and pulse-location take the values

$$\sigma_s^2 = \sqrt{D/\mu}, \quad a_s = -\frac{\Gamma}{2\mu\sigma_s^2}.$$

One of the fixed points corresponds to the trivial solution,

$$g_s = \alpha/\gamma, \quad \psi_s = 0,$$

while the other corresponds to the ground-mode pulse,

$$g_s = l + \mu a_s^2 + D/\sigma_s^2, \quad \psi_s^2 = \frac{\alpha - \gamma g_s}{\beta g_s \sqrt{\pi}\sigma_s}.$$

These agree precisely with the results derived in section 3.

6.1.1. Linear dynamics. Before discussing the general solution of the pulse-evolution equations, let us first reconsider the dynamics of transient linear pulse formation below threshold. If we linearize the pulse-amplitude and gain equations about the trivial solution ($\psi_s = 0$ and $g_s = \alpha/\gamma$), the result is

$$T_R \frac{d}{dT}\sigma^2 = 2\left(D - \mu\sigma^4\right), \tag{6.6}$$

$$T_R \frac{d}{dT}a = -\Gamma - 2\mu\sigma^2 a, \tag{6.7}$$

$$T_R \frac{d}{dT}\psi = \left(\frac{\alpha}{\gamma} - l - \mu a^2 - \frac{D}{\sigma^2}\right)\psi, \tag{6.8}$$

$$\frac{d}{dT}g = -\gamma g, \tag{6.9}$$

where $\psi(T)$ and $g(T)$ represent perturbations to the trivial solution. Note that the pulse-amplitude and gain are now decoupled. The perturbation to the steady-state gain dies off

on the time scale of $1/\gamma$, while the pulse-amplitude perturbation is driven only by the pulse-location and pulse-width.

In order to simplify the resulting analysis, let us assume that the pulse-width is in steady-state, i.e., $\sigma = \sigma_s$. Equation (6.7) is a nonhomogeneous first-order differential equation and has the solution

$$a(T) = a_s + (a_0 - a_s)\exp\left(-\frac{2\sqrt{\mu D}\,T}{T_R}\right), \tag{6.10}$$

where a_0 is the initial location of the pulse. The pulse therefore sweeps into position monotonically on a time scale of $T_R/2\sqrt{\mu D}$. Note that while the *velocity* of the pulse, da/dT, depends on its current location, it depends linearly on the detuning Γ, in agreement with the drift velocity findings of Morgner and Mitschke [27].

Recalling the definition of g_0, (3.9), the pulse-amplitude equation, (6.8), can be written as

$$T_R\frac{d}{dT}\psi = \left(\left(\frac{\alpha}{\gamma} - g_0\right) + \mu(a_s^2 - a^2)\right)\psi \tag{6.11}$$

and is therefore separable. An explicit solution in terms of T is possible, but it is more revealing to write the solution as a function of pulse-location $a(T)$,

$$\psi(T) = \psi_0\exp\left(\frac{(\alpha - \gamma g_0)T}{\gamma T_R}\right)\exp\left(\frac{(a(T)+a_s)^2 - (a_0+a_s)^2}{4\sigma_s^2}\right), \tag{6.12}$$

where ψ_0 is the initial amplitude of the pulse.

Let us first consider the linearized dynamics at threshold, in which case $\alpha = \gamma g_0$. The first exponential in (6.12) therefore drops out. Moreover, since $a(T)$ changes monotonically, we see that $\psi(T)$ must also change monotonically, and we also know that $\lim_{T\to\infty} a(T) = a_s$. Therefore,

$$\psi_s = \lim_{T\to\infty}\psi(T) = \psi_0\exp\left(\frac{4a_s^2 - (a_0+a_s)^2}{4\sigma_s^2}\right). \tag{6.13}$$

What then should the initial location of the pulse be in order to maximize the growth in pulse-amplitude? The quadratic nature in a_0 of the exponent above reveals that the optimum value is $a_0 = -a_s$, i.e., the adjoint location. In this case, the pulse experiences a growth of

$$\text{Growth} = \frac{\psi_s^2}{\psi_0^2} = \exp\left(\frac{2a_s^2}{\sigma_s^2}\right) = \exp(4\Delta^2), \tag{6.14}$$

which agrees with our results from section 5.

We can extend our analysis further by considering the transient growth below threshold, for which $\alpha < \gamma g_0$. In this case, the first exponential in (6.12) no longer vanishes but represents a decaying exponential function of T. Multiplication by the other exponential, which changes monotonically in T, shows that the growth experienced by a pulse below threshold is less than that at threshold. The maximum amplitude obtained by the pulse can be determined by finding the time T^* at which $\psi_T = 0$. Let us denote the pulse-amplitude and pulse-location

at this time as $\bar{\psi}$ and $\bar{a}$, respectively, i.e., $\bar{\psi} = \psi(T^*)$ and $\bar{a} = a(T^*)$. Then (6.11) shows that the maximum amplitude is obtained when

$$\left(\frac{\alpha}{\gamma} - g_0\right) + \mu\left(a_s^2 - \bar{a}^2\right) = 0. \tag{6.15}$$

If we denote $\alpha = \alpha_{th}(1-\varepsilon)$ so that ε represents the % below threshold, then the pulse-location corresponding to maximum amplitude is given by one of the roots of

$$\bar{a}^2 = a_s^2\left(1 - \frac{\varepsilon g_0}{\mu a_s^2}\right), \tag{6.16}$$

which shows that close to threshold the pulse-location decreases linearly with ε.

There are, of course, two solutions to (6.16). A simple calculation shows that one of these corresponds to a maximum amplitude and the other to a minimum amplitude. The maximum energy growth is therefore achieved if we place the initial pulse in the minimum location, i.e., $a_0 = -\bar{a}$. At threshold, this optimum pulse is just the adjoint pulse, but below threshold this optimum pulse is located closer to the origin as discussed in section 5.

The time T^* at which the maximum amplitude is obtained can now be determined from (6.10). If we assume that the pulse begins in the optimum location, $a_0 = -\bar{a}$, then

$$\frac{2\sqrt{\mu D}}{T_R}T^* = \ln\left(\frac{\varepsilon g_0}{\mu a_s^2}\right) - 2\ln\left(1 - \sqrt{1 - \frac{\varepsilon g_0}{\mu a_s^2}}\right). \tag{6.17}$$

The time taken to reach maximum energy therefore decreases according to $\ln(\varepsilon)$. The maximum energy can now be determined directly from (6.12) if we evaluate this expression with $T = T^*$, $a(T^*) = \bar{a}$, and $a_0 = -\bar{a}$. The result is

$$\ln\left(\frac{\bar{\psi}^2}{\psi_0^2}\right) = 4\Delta^2\sqrt{1 - \frac{\varepsilon g_0}{\mu a_s^2}} - \frac{2\varepsilon g_0 T^*}{T_R}, \tag{6.18}$$

which shows that the maximum energy obtained by the pulse below threshold is always less than that at threshold.

These results are summarized in Figure 6.1, in which we graph both the exact results obtained above (solid lines) and those from direct numerical simulation of the governing linearized PDE (symbols). In Figure 6.1(a) we show the maximum relative energy attained by the pulse as a function of ε, while in Figure 6.1(b) we show the time taken to achieve maximum relative energy versus ε. These results demonstrate that close to threshold the initial optimum pulse experiences growth on the order of $\exp(4\Delta^2)$, and that this growth shows a weak drop-off versus ε.

6.1.2. Nonlinear dynamics. Now let us consider the general solution of the pulse-parameter equations, (6.2)–(6.5). The equations for the pulse-width and pulse-location can be solved exactly. In the limit as $T \to \infty$ both σ and a approach their steady-state values, σ_s and a_s. In terms of the long-term behavior we can therefore consider the pulse-amplitude and gain equations with both the pulse-width and pulse-location in steady-state. Under these conditions

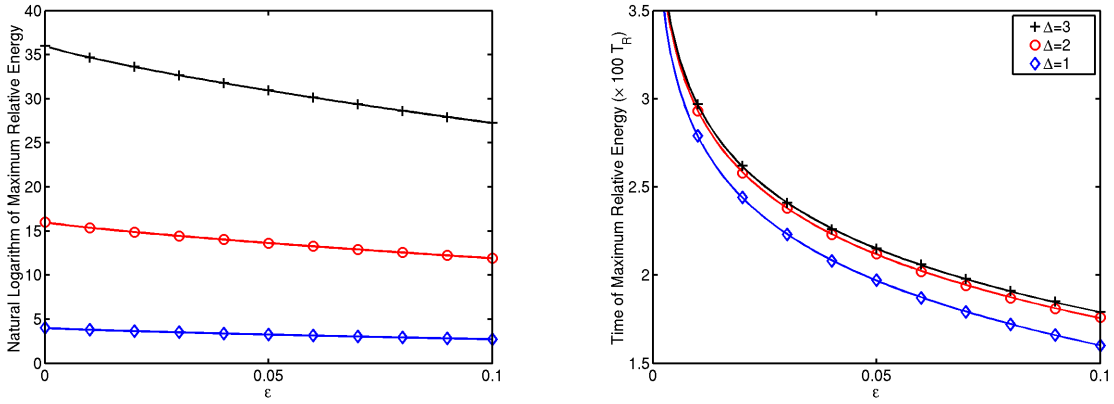

(a) (b)

Figure 6.1. *Transient growth of an optimal perturbation to the trivial solution below threshold:* (a) *Natural logarithm of the maximum relative pulse energy versus percentage below threshold;* (b) *time taken to reach maximum relative energy versus percentage below threshold.*

the equations are

$$T_R \frac{d}{dT}\psi = (g - g_0)\psi, \tag{6.19}$$

$$\frac{d}{dT}g = \alpha - \gamma g - \sqrt{\pi}\beta\sigma_s g\psi^2. \tag{6.20}$$

It is convenient at this stage to use the pulse-energy $E = \sqrt{\pi}\sigma_s\psi^2$ and rewrite the equations as

$$E_T = 2\frac{(g - g_0)}{T_R}E, \tag{6.21}$$

$$g_T = \alpha - \gamma g - \beta g E. \tag{6.22}$$

This system represents a set of nonlinear differential equations in the plane. As a result, there is a limited number of solutions available, including evolution to a fixed point and limit cycles [14]. As we already know, the fixed point corresponding to the trivial solution, $g = \alpha/\gamma$, $E = 0$, exists for all α, is linearly stable for $\alpha < \alpha_{th}$, and is linearly unstable for $\alpha > \alpha_{th}$. In addition, the fixed point corresponding to the ground-mode lasing solution, $g = g_0$, $E = (\alpha - \gamma g_0)/\beta g_0$, exists only if $\alpha > \alpha_{th}$ and is linearly stable there. In what follows we will show that closed orbits are not possible. The system therefore evolves so as to collapse onto the appropriate fixed point. Below threshold this is the trivial solution, while above threshold this is the ground-mode lasing solution.

In order to rule out the existence of closed orbits, we will make use of *Dulac's criterion* [14] in the first quadrant, $E > 0, g > 0$. In this context, Dulac's criterion amounts to finding a continuously differentiable real-valued function $u(E, g)$ such that $\partial_E(u(E, g)E_T) + \partial_g(u(E, g)g_T)$ is of one sign throughout the first quadrant. It suffices to choose $u(E, g) = 1/Eg$, and we find

that

$$\begin{aligned}\partial_E(u(E,g)E_T)+\partial_g(u(E,g)g_T) &= \partial_E\left(2\frac{(g-g_0)}{T_R E g}E\right)+\partial_g\left(\frac{(\alpha-\gamma g-\beta g E)}{Eg}\right)\\ &= \partial_E\left(2\frac{(g-g_0)}{T_R g}\right)+\partial_g\left(\frac{\alpha}{Eg}-\frac{\gamma}{E}-\beta\right)\\ &= 0+\partial_g\left(\frac{\alpha}{Eg}\right)\\ &= -\frac{\alpha}{Eg^2}\\ &< 0 \quad \text{in the first quadrant.}\end{aligned}$$

There are therefore no closed orbits in the first quadrant, and the system must collapse onto the appropriate fixed point.

In order to confirm these predictions, we have run simulations of the governing ODEs (6.2)–(6.5) both above and below threshold. In Figures 6.2 and 6.3 we show the results for the case of $\Delta = 3$. The initial conditions correspond to the pulse-width in steady-state ($\sigma(0) = \sigma_s$), the pulse-location in the optimum location ($a(0) = -\bar{a}$), an initial pulse amplitude of 10^{-8}, and an initial gain of g_0.

In Figure 6.2(a)–(d) we show the results when we operate at 5% below threshold. Figure 6.2(a) shows that the pulse sweeps into position exponentially with T, as expected from (6.10). For these parameter values, our linear analysis suggests that we should see amplitude growth on the order of $\exp(2\Delta^2) \approx 6.5 \times 10^7$ and that the maximum amplitude should be reached when $T \approx 2.2 \times 100 T_R$. Figure 6.2(c) shows that this is still true in the presence of the nonlinear coupling between the gain and the pulse-amplitude. The gain dynamics are shown in Figure 6.2(b). After initially decaying, the gain rebounds and assumes its equilibrium value of $\alpha/\gamma = 0.1805$. In Figure 6.2(d) we show the corresponding contour plot of the nonlinear pulse formation process, reconstructed from the ODE simulation.

In Figure 6.3(a)–(b) we show the pulse-amplitude dynamics when we operate the laser at 5% above threshold. After it overshoots its mark, the pulse-amplitude oscillates briefly before reaching its equilibrium value of $\psi_0 \approx 0.168$. The contour plot of the pulse evolution is shown in Figure 6.3(b).

6.2. Single pulse and noise. In the previous section we showed that, above threshold, an initial optimum pulse evolves nonlinearly into a ground-mode pulse. In the early stages of its evolution it experiences large energy growth on the order of $\exp(4\Delta^2)$. After it has swept into position, the nonlinear interaction between the pulse amplitude and the gain arrests this growth and allows a ground-mode pulse of the correct energy to form.

The linear stability of this ground-mode pulse was addressed earlier. We showed that perturbations to the ground-mode pulse can experience similar levels of linear transient growth. In the presence of the nonlinearity the question of the outcome of these perturbations arises. In order to answer this question we have run a series of full PDE simulations. Our algorithm is based on a spectral Hermite approximation, as detailed in [2]. In the results that follow, we used 128 spectral modes and a time step of 0.01. Unless stated otherwise, all parameters are set to those given in section 2.

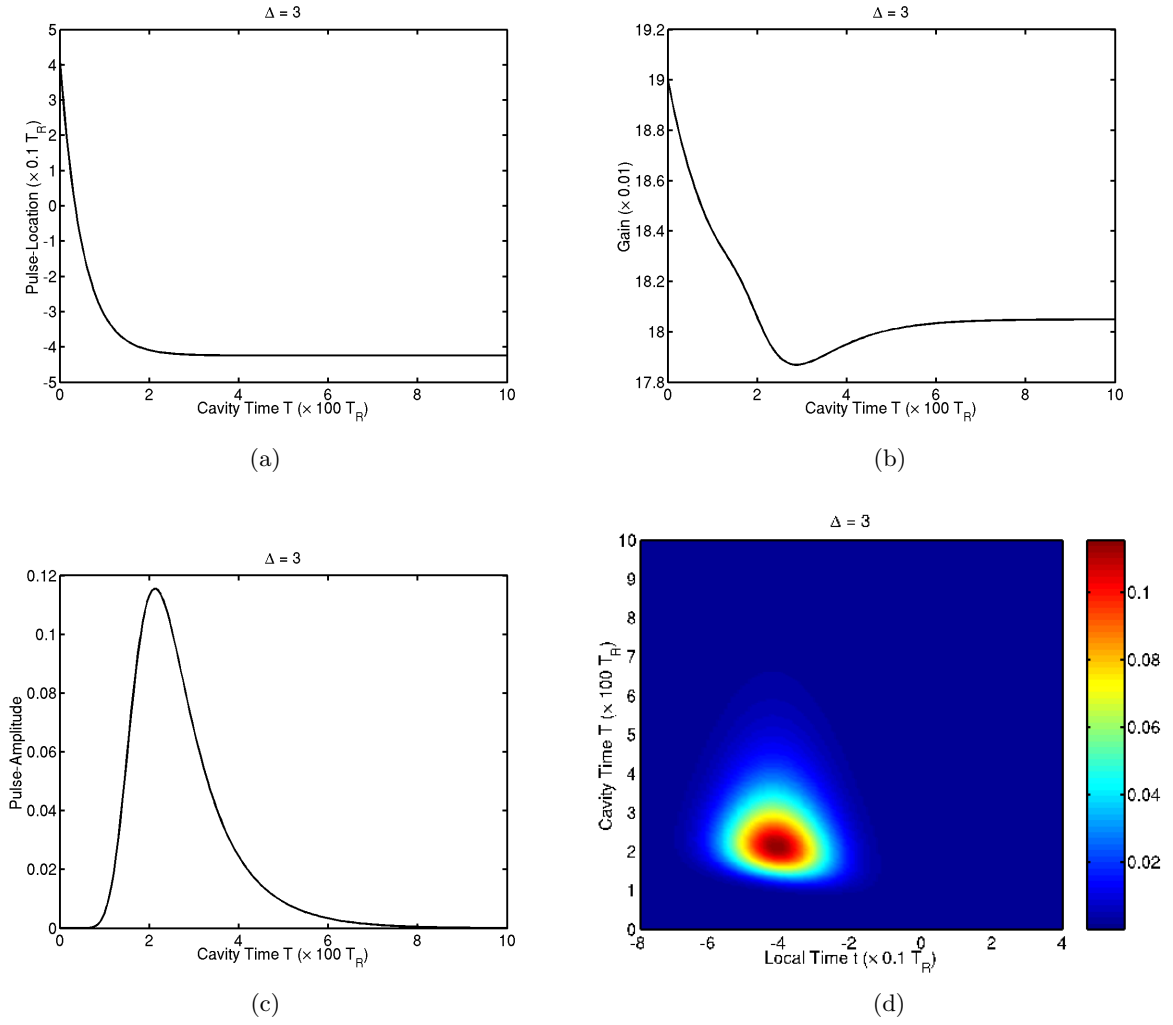

Figure 6.2. *Nonlinear evolution of a pulse at* 5% *below threshold for* $\Delta = 3$ *as governed by* (6.2)–(6.5). (a) *Pulse-location,* (b) *gain,* (c) *pulse-amplitude, and* (d) *contour plot of the pulse amplitude. The initial conditions correspond to an optimum pulse of equilibrium width and amplitude* 10^{-8} *and an initial gain of* g_0.

In the first set of simulations, we consider the nonlinear interaction between a ground-mode pulse and a single perturbation pulse which initially occupies the adjoint location. In Figure 6.4 we show the results of a simulation for the case of $\Delta = 3$ at 5% above threshold. The adjoint pulse has an initial amplitude of 10^{-8} and is injected at $T = 10 \times 100T_R$. In Figure 6.4(a) we show the energy in the cavity as a function of T. The amplitude of the noise pulse grows very quickly as it sweeps across the domain and, by the time it arrives in position, its amplitude is comparable to that of the existing ground-mode pulse! It then begins to interact with the ground-mode pulse, and out of this interaction emerges a new ground-mode pulse, as shown in Figure 6.4(b). After some relaxation oscillations, the new ground-mode pulse settles into equilibrium.

In the second set of simulations, we consider the full nonlinear dynamics (2.1)–(2.2) in

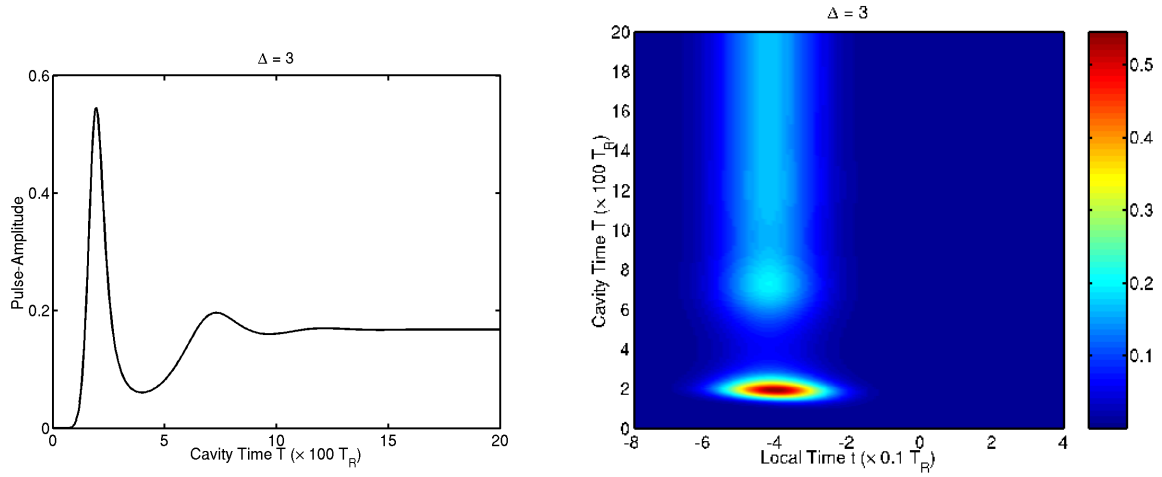

(a) (b)

Figure 6.3. *Nonlinear evolution of a pulse at* 5% *above threshold for* $\Delta = 3$ *as governed by* (6.2)–(6.5). (a) *Pulse-amplitude and* (b) *contour plot of the pulse amplitude. The initial conditions correspond to an optimum pulse of equilibrium width and amplitude* 10^{-8} *and an initial gain of* g_0.

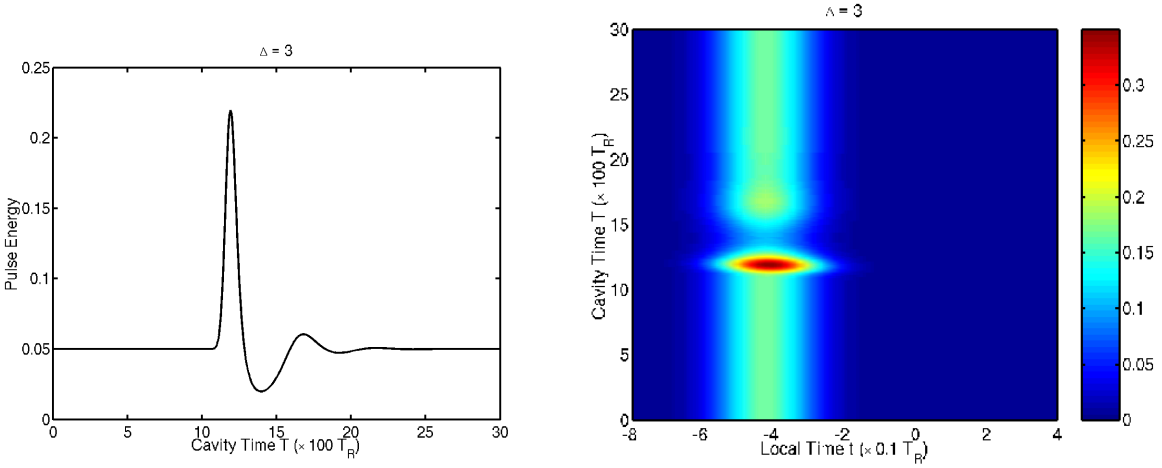

(a) (b)

Figure 6.4. *Pulse-dynamics at* 5% *above threshold for* $\Delta = 3$ *as governed by* (2.1)–(2.2). (a) *Pulse-energy and* (b) *contour plot of the pulse-amplitude. With the pulse-amplitude and gain in equilibrium, a single adjoint noise pulse of amplitude* 10^{-8} *is injected at* $T = 10 \times 100 T_R$.

the presence of stochastic noise. Our noise source is white with an amplitude of 10^{-8}. In Figure 6.5 we show the results of a simulation for $\Delta = 3$ at 5% above threshold. Figure 6.5(a) shows the energy in the cavity as a function of T, while Figure 6.5(b) shows the contour plot of the pulse-amplitude.

Figure 6.5 suggests that in the presence of a continuous noise source, the process of adjoint noise pulse growth occurs over and over again in the following sense. Out of the noise

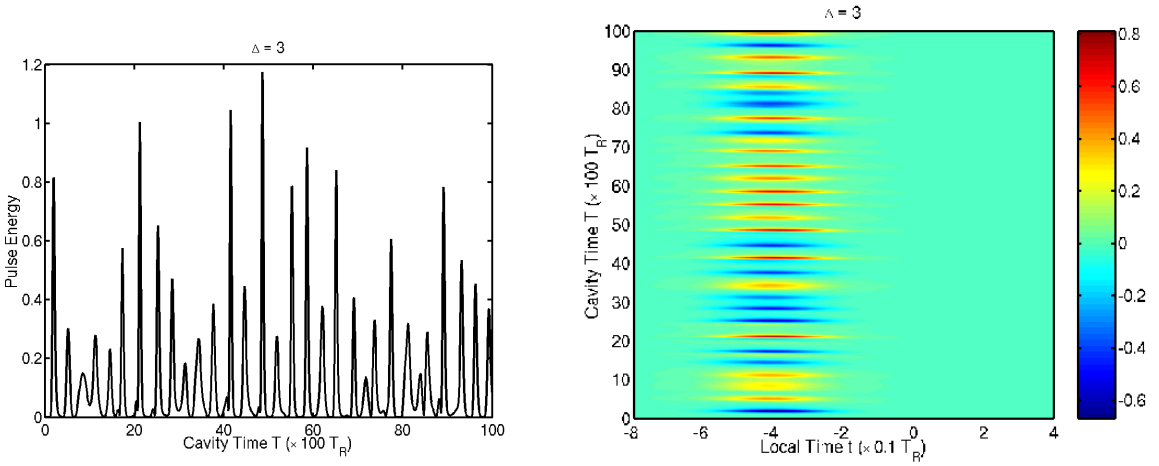

(a) (b)

Figure 6.5. *Pulse dynamics at* 5% *above threshold for* $\Delta = 3$ *as governed by* (2.1)–(2.2) *in the presence of white noise of amplitude* 10^{-8}. (a) *Pulse-energy and* (b) *contour plot of* $A(T, t)$.

spectrum, a pulse that begins in the adjoint location dominates as it experiences the most transient growth. As it grows and sweeps into position, it begins to compete with an existing ground-mode pulse. Out of this interaction emerges a new ground-mode pulse, which is now susceptible to the growth of another adjoint pulse. This process then repeats endlessly, with the time between successive pulses dictated by the transient growth time.

7. Conclusion. In this paper we have considered the linear and nonlinear dynamics of pulse formation in an actively mode-locked laser. The trivial solution of the laser equations loses stability at the lasing threshold to an off-center Gaussian pulse. The delay in the laser pulse with respect to the minimum loss point is proportional to the normalized modulator detuning Δ. The lowest-order Hermite–Gaussian mode is linearly stable to perturbations, while the higher-order modes are linearly unstable to the lower-order modes. One would therefore expect that at threshold the laser would turn on and emit stable ground-mode laser pulses.

As a result of the nonnormality of the linear operator, however, the laser is subject to large transient growth on the order of $\exp(4\Delta^2)$ at the lasing threshold, in agreement with previous findings by Kärtner, Zumbühl, and Matuschek [21]. We also find that the transient growth at threshold is precisely the Petermann excess noise factor [30, 34, 35] for a laser governed by a nonnormal operator. Below threshold we found exact expressions for the transient growth, and we showed that the perturbation which experiences maximum growth is closely related to the adjoint laser mode.

Our reduction of the governing PDEs to a low-dimensional system of ODEs for an evolving pulse is novel. It provides us with an insight into the pulse formation dynamics. The linearized version allowed us to determine exact results on transient growth, such as the maximum energy attained and the time taken to reach maximum energy. We also showed that the nonlinear system collapses onto the appropriate fixed point and that no limit cycles are possible. In the

absence of a continuous noise source, there are no interesting dynamics; an initial perturbation grows and sweeps into position and is stable there. In the presence of noise, however, the laser effectively destabilizes as new laser pulses are repeatedly formed out of the noise spectrum.

The importance of nonnormal operators is well known to both the fluids [38] and optics [35] communities. In viscous shear flow, much of the focus has been on the transient growth experienced by a single perturbation; the resulting dynamics are often a matter of conjecture, although simple models have been proposed which couple transient growth and nonlinear mixing [13]. In laser physics, the presence of a stochastic noise source, in the form of spontaneous emission noise, is vital for laser operation. The Petermann excess noise factor is a measure of the influence that the nonorthogonal laser modes have on the strength of the noise source. At the lasing threshold, these two factors—transient growth and excess noise—are identical. This results from the fact that the transient growth experienced at threshold is determined by the projection of the initial perturbation onto the ground-mode laser pulse. If the initial perturbation is the adjoint laser mode, then this is precisely the excess noise factor.

Comparable results have been reported by Longhi and Laporta [26] in the context of a frequency-modulated laser. The results obtained here could be extended to cover the frequency-modulated case by allowing the modulation parameter μ to become complex. In addition, an immediate extension of the work presented here would be to spatio-temporal as opposed to temporal laser pulses. In this case, Dunlop, Firth, and Wright [9] have derived the appropriate spatio-temporal master equation that describes pulse formation and have applied it to a Kerr lens mode-locked laser. Allowing for both AM and FM and including both space and time in the laser operator would represent a complete generalization of the model studied here.

Acknowledgments. We thank the referees for their excellent feedback, particularly the comments relating to the optimal growth curves.

REFERENCES

[1] G. Bachman and L. Narici, *Functional Analysis*, Academic Press, New York, 1966.
[2] K. Black and J. B. Geddes, *Spectral Hermite approximations for the actively mode-locked laser*, J. Sci. Comput., 16 (2001), pp. 81–120.
[3] M. H. Crowell, *Characteristics of mode-coupled lasers*, IEEE J. Quantum. Electronics, 1 (1965), pp. 12–20.
[4] T. Deutsch, *Mode-locking effects in an internally modulated ruby laser*, Appl. Phys. Lett., 7 (1965), pp. 80–82.
[5] M. DiDomenico, *Small-signal analysis of internal (coupling type) modulation of lasers*, J. Appl. Phys., 35 (1964), pp. 2870–2876.
[6] M. DiDomenico, H. M. Marcos, J. E. Geusic, and R. E. Smith, *Generation of ultrashort optical pulses by mode locking the YAG:Nd laser*, Appl. Phys. Lett., 8 (1966), pp. 180–183.
[7] A. J. DeMaria and D. A. Stetser, *Laser pulse-shaping and mode-locking with acoustic waves*, Appl. Phys. Lett., 7 (1965), pp. 71–73.
[8] A. J. DeMaria, D. A. Stetser, and H. Heynau, *Self mode-locking of lasers with saturable absorbers*, Appl. Phys. Lett., 8 (1966), pp. 174–176.
[9] A. M. Dunlop, W. J. Firth, and E. M. Wright, *Master equation for spatio-temporal beam propagation and Kerr lens mode-locking*, Opt. Comm., 138 (1997), pp. 211–226.
[10] A. M. Dunlop, W. J. Firth, and E. M. Wright, *Time-domain master equation for pulse evolution and laser mode-locking*, Opt. Quantum Electronics, 32 (2000), pp. 1131–1146.

[11] B. F. Farrell, *Optimal excitation of perturbations in viscous shear flow*, Phys. Fluids, 31 (1988), pp. 2093–2102.
[12] B. F. Farrell and P. J. Ioannou, *Stochastic forcing of the linearized Navier-Stokes equations*, Phys. Fluids A, 5 (1993), pp. 2600–2609.
[13] T. Gebhardt and S. Grossmann, *Chaos transition despite linear stability*, Phys. Rev. E (3), 50 (1994), pp. 3705–3711.
[14] J. Guckenheimer and P. Holmes, *Nonlinear Oscillations, Dynamical Systems, and Bifurcations of Vector Fields*, Appl. Math. Sci. 42, Springer-Verlag, New York, 1983.
[15] H. Haken and M. Pauthier, *Nonlinear theory of multi-mode action in loss modulated lasers*, IEEE J. Quantum Electronics, 4 (1968), pp. 454–459.
[16] L. E. Hargrove, R. L. Fork, and M. A. Pollack, *Locking of He-Ne laser modes induced by synchronous intracavity modulation*, Appl. Phys. Lett., 5 (1964), pp. 4–5.
[17] S. E. Harris and R. Targ, *Fm oscillation of the He-Ne laser*, Appl. Phys. Lett., 5 (1964), pp. 202–204.
[18] S. E. Harris and O. P. McDuff, *Theory of FM laser oscillation*, IEEE J. Quantum Electronics, 1 (1965), pp. 245–262.
[19] H. A. Haus, *A Theory of Forced Mode Locking*, IEEE J. Quantum Electronics, 11 (1975), pp. 323–330.
[20] J. M. Hopkins and W. Sibbett, *Ultra-short pulse lasers: Big payoffs in a flash*, Scientific American, 283 (2000), pp. 72–79.
[21] F. X. Kärtner, D. M. Zumbühl, and N. Matuschek, *Turbulence in mode-locked lasers*, Phys. Rev. Lett., 82 (1999), pp. 4428–4431.
[22] D. M. Kim, S. Marathe, and T. A. Rabson, *Eigenfunction analysis of mode-locking process*, J. Appl. Phys., 44 (1973), pp. 1673–1675.
[23] D. J. Kuizenga and A. E. Siegman, *FM and AM mode-locking of the homogeneous laser* I: *Theory*, IEEE J. Quantum Electronics, 6 (1970), pp. 694–708.
[24] D. J. Kuizenga and A. E. Siegman, *FM and AM mode-locking of the homogeneous laser* II: *Experimental results*, IEEE J. Quantum Electronics, 6 (1970), pp. 709–715.
[25] W. E. Lamb Jr., *Theory of an optical laser*, Phys. Rev., 134 (1964), pp. A1429–A1450.
[26] S. Longhi and P. Laporta, *Excess noise in intracavity laser frequency modulation*, Phys. Rev. E. (3), 61 (2000), pp. R989–R992.
[27] U. Morgner and F. Mitschke, *Drift instabilities in the pulses from cw mode-locked lasers*, Phys. Rev. E. (3), 58 (1998), pp. 187–192.
[28] P. M. Morse and H. Feshbach, *Methods of Theoretical Physics, Vol.* 1, McGraw–Hill, New York, 1953.
[29] T. J. Nelson, *A coupled-mode analysis of mode locking in homogeneously broadened lasers*, IEEE J. Quantum Electronics, 8 (1972), pp. 29–33.
[30] K. Petermann, *Calculated spontaneous emission factor for double-heterostructure injection lasers with gain-induced waveguiding*, IEEE J. Quantum Electronics, 15 (1979), pp. 566–570.
[31] S. C. Reddy and D. S. Henningson, *Energy growth in viscous channel flows*, J. Fluid Mech., 252 (1993), pp. 209–238.
[32] P. J. Schmid and D. S. Henningson, *Stability and Transition in Shear Flows*, Appl. Math. Sci. 142, Springer-Verlag, New York, 2001.
[33] A. E. Siegman, *Lasers*, University Science Books, Sausalito, CA, 1986.
[34] A. E. Siegman, *Excess spontaneous emission in non-Hermitian optical systems.* I. *Laser amplifiers*, Phys. Rev. A, 39 (1989), pp. 1253–1263.
[35] A. E. Siegman, *Excess spontaneous emission in non-Hermitian optical systems.* II. *Laser oscillators*, Phys. Rev. A, 39 (1989), pp. 1264–1268.
[36] P. W. Smith, T. J. Bridges, E. G. Burkhardt, and O. R. Wood, *Mode-locked high pressure waveguide CO_2 laser*, Appl. Phys. Lett., 21 (1972), pp. 470–472.
[37] G. Stix, *The triumph of the light*, Scientific American, 284 (2001), pp. 80–87.
[38] L. N. Trefethen, A. E. Trefethen, S. C. Reddy, and T. A. Driscoll, *Hydrodynamic stability without eigenvalues*, Science, 261 (1993), pp. 578–584.
[39] A. M. van der Lee, A. L. Mieremet, M. P. van Exter, N. J. van Druten, and J. P. Woerdman, *Quantum noise in a laser with nonorthogonal polarization modes*, Phys. Rev. A, 61 (2000), 033812.